Progress of Theoretical Physics, Vol. 72, No. 5, November 1984

Stability Theory of Synchronized Motion in Coupled-Oscillator Systems. III

—— *Mapping Model for Continuous System* ——

Tomoji YAMADA and Hirokazu FUJISAKA*

Department of Physics, Kyushu Institute of Technology, Kitakyushu 804
**Department of Physics, Kagoshima University, Kagoshima 890*

(Received May 12, 1984)

By starting with a reaction-diffusion equation a mapping model for the continuous system is proposed. The transition from the uniform state to the non-uniform one occurs at the same value of the diffusion constant for the mapping model as for the original reaction-diffusion equation if the transition exists. The mapping model is further studied by adopting the logistic model in one-dimensional space with a periodic boundary condition. Equal time spectra in wave number space and power spectra for several values of wave numbers are numerically obtained. A comparison of the numerical results of the equal time spectra with a simple theory is made to give a satisfactory agreement for large wave numbers.

§ 1. Introduction

The theoretical studies of chaos based on the dynamical mapping have been developed since May's work[1] and are found to be useful even in the analysis of real experiments.[2] In a usual situation, however, the time evolution of dynamical system is governed by a set of differential equations. Several works[3] have been done to obtain the mapping models from the original differential equations in the cases of low dimensional mappings. It is known that the appearance of the mapping reflects the existence of low dimensional attractor.

In a previous paper[4] of this series (hereafter referred to as II), we have developed a mapping theory of the coupled-oscillator system and obtained a dynamical mapping which describes the time evolution of the dynamical variables. The numerical calculations based on this mapping give similar results to those obtained from the original differential equations.[4] The advantages of the mapping theory are that (i) various results of the mapping theory can be used and (ii) the numerical computation becomes considerably easier.

One of physical significances of the coupled-oscillator system is in the introduction of the spatial degrees of freedom. Studies of the coupled-oscillator system by the mapping have been mainly carried out for the systems with a small number of oscillators.[5] Recently Deissler and Kaneko examined the system with a large number of oscillators.[6] Various new phenomena can be expected for this system. The study of spatial non-uniform system is interesting in connection with turbulence. In the present work we will extend the formulation in II to deal with the continuous system which can be considered to be an infinite number limit of the coupled-oscillator system.

We consider the following reaction-diffusion equation:

$$\dot{\boldsymbol{x}}=\boldsymbol{f}(\boldsymbol{x};\ t)+D\nabla^2\boldsymbol{x}\,, \tag{1·1}$$

where $\boldsymbol{x}$ and D are the state vector and the diffusion constant, respectively. As in II the

Downloaded from https://academic.oup.com/ptp/article/72/5/885/1927016 by guest on 20 August 2022

flow $\boldsymbol{f}$ has the periodic time dependence with respect to the time variable t as follows:

$$\boldsymbol{f}(\boldsymbol{x};\ t+T)=\boldsymbol{f}(\boldsymbol{x};\ t), \tag{1·2}$$

where T is an integer multiple of the period of the external field. The same types of equations as (1·1) have been studied by several authors.[7] As in II we assume that (1·1) has the mapping,

$$\boldsymbol{x}_{n+1}=\boldsymbol{g}(\boldsymbol{x}_n), \tag{1·3}$$

in the absence of the diffusion term, where $\boldsymbol{x}_n$ is the state vector at time $t=nT(n=0, 1, 2, \cdots)$.

The mapping function for the continuous system (1·1) is obtained in terms of (1·3) in §2. The Lyapunov exponent in the uniform state is discussed in §3 by using the mapping function. In §4 numerical calculations are carried out on the mapping in one-dimensional space by adopting the logistic model.[1] Section 5 is devoted to the summary and some remarks.

§ 2. Mapping function

The continuos system (1·1) is studied by extending the formulation given in II.[4] By introducing the new state vector $\boldsymbol{y}$ as

$$\boldsymbol{y}=\exp\{-D(t-t_n)\nabla^2\}\boldsymbol{x}\,, \tag{2·1}$$

Eq. (1·1) becomes

$$\dot{\boldsymbol{y}}=\exp\{-D(t-t_n)\nabla^2\}\boldsymbol{f}(\boldsymbol{x};\ t). \tag{2·2}$$

We define the following quantity

$$|\delta\boldsymbol{y}|=l\overline{|\nabla y_\alpha|}\,, \tag{2·3}$$

where the notation $\overline{(\cdots)}$ denotes the spatial average, l is the diffusion characteristic length $l\equiv\sqrt{DT}$ and y_α denotes the α-th component of $\boldsymbol{y}$. It measures the magnitude of $l|\nabla y_\alpha|$ and assumed to be small. (See Appendix A for the details). As is shown in Appendix A, Eq. (2·2) can be written as

$$\dot{\boldsymbol{y}}=\boldsymbol{f}(\boldsymbol{y};\ t)+O(|\delta\boldsymbol{y}|^2). \tag{2·4}$$

If we discard the second order terms with respect to $|\delta\boldsymbol{y}|$ in (2·4), Eq. (2·4) has the same form as Eq. (1·1) without the diffusion term and, therefore from the assumption (1·3) we have

$$\boldsymbol{y}_{n+1}=\boldsymbol{g}(\boldsymbol{y}_n), \tag{2·5}$$

where $\boldsymbol{y}_n$ is the state vector at $t=t_n\equiv nT$. Since $\boldsymbol{y}_n=\boldsymbol{x}_n$, we get

$$\boldsymbol{x}_{n+1}=\exp(\alpha\nabla^2)\boldsymbol{g}(\boldsymbol{x}_n) \tag{2·6}$$

with $\alpha=DT$, where $\boldsymbol{x}_n$ is the state vector $\boldsymbol{x}$ at $t=t_n$.

For the derivation of (2·6) we have neglected the second order terms with respect to $|\delta\boldsymbol{y}|$. Therefore, other form instead of (2·6) may be also possible. However, we adopt

Downloaded from https://academic.oup.com/ptp/article/72/5/885/1927016 by guest on 20 August 2022

Eq. (2·6) as the mapping model, since it gives a correct transition point from the uniform state to the non-uniform one as is shown in the next section.

§ 3. Stability of uniform state

In this section we examine the stability of the uniform state Ψ_{unif}. Let us imagine that the reference system is contained in a d-dimensional cube with the length of side L. The periodic boundary condition is assumed and the state vector in the uniform state is denoted as $\boldsymbol{x}_0(t)$. As was discussed in Ref. 8), hereafter referred to as I, the stability of the uniform state Ψ_{unif} is determined by the largest eigenvalue of the following matrix:

$$\begin{aligned}\hat{\Lambda}_{\boldsymbol{k}} &= \lim_{t\to\infty} t^{-1} \ln \exp_+\left[\int_0^t \{\hat{F}(s) - Dk^2\hat{1}\}ds\right] \\ &= \hat{\Lambda}_{k=0} - Dk^2\hat{1}\,, \end{aligned} \tag{3·1}$$

where $\hat{F}(t) = \partial \boldsymbol{f}(\boldsymbol{x}_0(t);\, t)/\partial \boldsymbol{x}_0(t)$, $\boldsymbol{k}$ is the wave vector ($k = |\boldsymbol{k}|$), and $\hat{1}$ is the unit matrix. The largest eigenvalue of $\hat{\Lambda}_{\boldsymbol{k}}$ is

$$\lambda_{\boldsymbol{k}}' = \lambda_{\text{L}} - Dk^2\,, \tag{3·2}$$

where λ_{L} is the largest Lyapunov exponent in Ψ_{unif}.

Next we consider the same problem by starting with Eq. (2·6). The uniform oscillation $\boldsymbol{x}_{0n}$ satisfies

$$\boldsymbol{x}_{0n+1} = \boldsymbol{g}(\boldsymbol{x}_{0n}). \tag{3·3}$$

Then, expanding the state vector around $\boldsymbol{x}_{0n}$, we have up to the first order in $\delta\boldsymbol{x}$:

$$\delta\boldsymbol{x}_{n+1} = \exp(\alpha \nabla^2)\hat{G}_n \delta\boldsymbol{x}_n\,, \tag{3·4}$$

where $\delta\boldsymbol{x}_n = \boldsymbol{x}_n - \boldsymbol{x}_{0n}$ and $\hat{G}_n = \partial \boldsymbol{g}(\boldsymbol{x}_{0n})/\partial \boldsymbol{x}_{0n}$. Denoting the spatial Fourier component of $\delta\boldsymbol{x}_n$ as $\delta\hat{\boldsymbol{x}}_n(\boldsymbol{k})$ we obtain

$$\delta\hat{\boldsymbol{x}}_n(\boldsymbol{k}) = \exp(-n\alpha k^2) \prod_{j=0}^{n-1}{}_+ \hat{G}_j \delta\hat{\boldsymbol{x}}_0(\boldsymbol{k}), \tag{3·5}$$

where $\prod_+$ denotes the ordered product. Therefore, if the largest eigenvalue of the matrix,

$$\begin{aligned}\hat{\Gamma}_{\boldsymbol{k}} &= \lim_{n\to\infty} \frac{1}{n} \ln\left[\exp(-n\alpha k^2) \prod_{j=0}^{n-1}{}_+ \hat{G}_j\right] \\ &= \hat{\Gamma}_{k=0} - \alpha k^2 \hat{1}\,, \end{aligned} \tag{3·6}$$

has a positive value for a certain region of the wave numbers, the uniform state becomes unstable. If the variable t in (3·1) is put equal to nT and the limit is taken as $n\to\infty$, from the definition of the mapping it is obvious that $\hat{\Gamma}_0$ is equivalent to $T\hat{\Lambda}_0$ since $\boldsymbol{x}_{0n}$, which is the solution of $\dot{\boldsymbol{x}}_0(t) = \boldsymbol{f}(\boldsymbol{x}_0(t);\, t)$ at time $t = t_n$, is assumed to be eventually described by Eq. (3·3). Therefore the largest eigenvalue of the matrix $\hat{\Gamma}_{\boldsymbol{k}}$ is given by

$$\gamma_{\boldsymbol{k}}' = T\lambda_{\text{L}} - \alpha k^2 = T\lambda_{\boldsymbol{k}}'\,. \tag{3·7}$$

As the smallest value of k^2 is $(2\pi/L)^2$, the uniform state loses its stability for

Downloaded from https://academic.oup.com/ptp/article/72/5/885/1927016 by guest on 20 August 2022

$$D<D_c=\lambda_L(L/2\pi)^2 \tag{3·8}$$

in both systems described by (1·1) and (2·6), if $\lambda_L>0$. It is clear from (3·8) that for the chaotic uniform state where $\lambda_L>0$ the non-uniform state appears for $D<D_c$ and the modes with $k<k_C=\sqrt{\lambda_L/D}$ grow from the initially uniform state.

§ 4. Mapping model for the continuous system

The mapping model (2·6) is obtained under the condition that the spatial variations of the state vectors are not large. This condition may be satisfied if the Lyapunov exponent is sufficiently small or the system is near the instability point discussed in §3. Thus it depends on various system parameters whether the mapping model is useful or not in a realistic system.

In order to examine the properties of the mapping model (2·6) we consider the simple case where the mapping function is further reduced to be one-dimensional. For this purpose we adopt the logistic model[1] as the mapping function and assume the space dimension to be one. We start with the following equation,

$$x_{n+1}(r)=\exp(\alpha\partial^2/\partial r^2)g(x_n(r)), \qquad n=0, 1, 2, \cdots, \tag{4·1}$$

where

$$g(x)=ax(1-x) \tag{4·2}$$

and $x_n(r)$ denotes the n-th iterated value of the state variable (one component of the state vector at time $t=nT$) at the position r. We assume the following periodic boundary condition:

$$x_n(r+L)=x_n(r), \tag{4·3}$$

where L is the system size. It is easily seen from (4·1) that the transformations, $\alpha\to\alpha s^2$, $L\to sL$ with the scale facter s yield an equivalent system to the original one.

The numerical calculation is carried out for $L=2\pi$ by dividing the space into M spatial mesh points with $M=1024$. Thus the spatial Fourier transform can be written as

$$\hat{x}_n(k)=\int_0^L e^{ikr}x_n(r)dr$$

$$=\Delta r\sum_{j=1}^{M}e^{ikr_j}x_n(r_j) \tag{4·4}$$

with $\Delta r=L/M$ and $r_j=j\Delta r$. The parameter α is fixed to be 10^{-4} and the initial condition is taken to be

$$x_{n=0}(r_j)=0.1+0.8\times\{\sqrt{3}j\}, \tag{4·5}$$

where $\{\cdots\}$ is the operator to take the

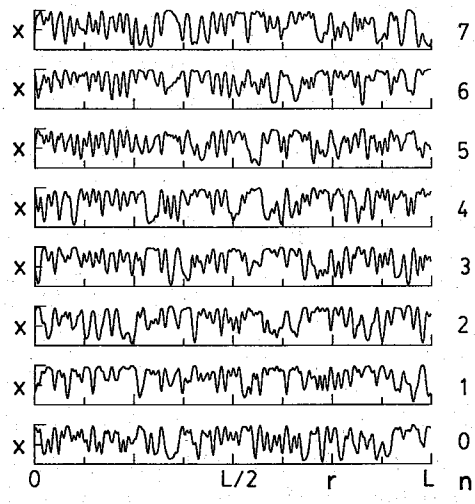

Fig. 1. The spatial variation of $x_n(r)$ for successive values of n. The parameter a is 4.0 and the origin of time $n=0$ is set after a sufficiently large number of initial steps. The symbol x stands for $x_n(r)$ and the interval of the vertical axis is from 0 to 1.

Downloaded from https://academic.oup.com/ptp/article/72/5/885/1927016 by guest on 20 August 2022

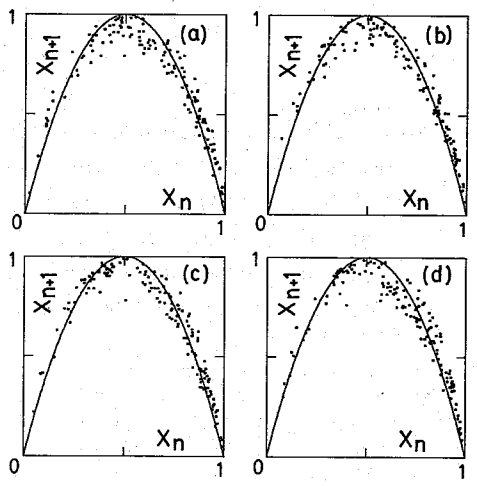

Fig. 2. The iterated mappings, $x_n(r) \to x_{n+1}(r)$, at (a) $r=0$, (b) $r=L/4$, (c) $r=L/2$, (d) $r=3L/4$. For simplicity, in these figures the argument r is not written and 150 iterated points are plotted. The full line denotes the mapping function $g(x) = ax(1-x)$.

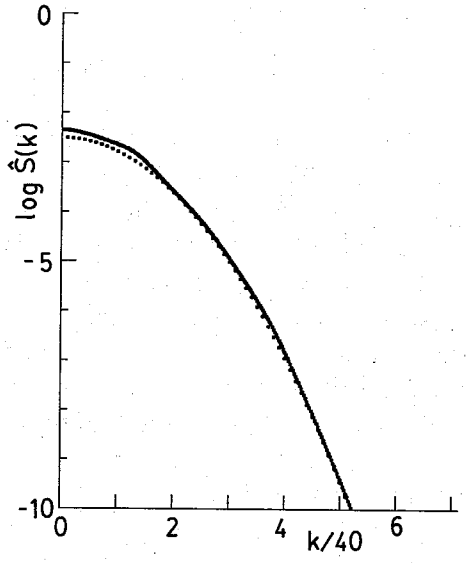

Fig. 3. The equal time spectrum for $a=4.0$. The full line denotes the numerical values and the dotted smooth curve is calculated from the theoretical equation (4·7). The function log means the common logarithm.

decimal part. After a sufficiently large number of initial steps we have an aged system which shows a stationary time behavior. The iteration procedure is carried out by using the FFT method (the fast Fourier transform) twice at each step.

In Fig. 1 the time evolution of the state variable $x_n(r)$ is plotted for $a=4$. The spatial patterns apparently show chaotic behaviors. Since the Lyapunov exponent λ_L of the logistic model for $a=4$ is $\ln 2 \fallingdotseq 0.6931$, the characteristic wave number k_c defined in §3 is $\sqrt{\lambda_L/a} \fallingdotseq 83.3$. In order to see the time evolution of $x_n(r)$, $\{x_n(r)\}$ $(n=1, 2, \cdots, 150)$ at $r=0$, $L/4$, $L/2$, $3L/4$ are shown in Fig. 2 in the forms of the mappings, $x_n(r) \to x_{n+1}(r)$. The points are scattered over a wide range and no periodic behavior is observed. The averaged value $\langle \hat{x}_n(0) \rangle / L$ is about 0.6596, where the brackets denote the time average.

The spatial correlation is reflected in the equal time spectrum defined by

$$\hat{S}(k) = \lim_{N\to\infty} \frac{1}{N} \sum_{n=1}^{N} \hat{x}_n(k) \hat{x}_n^*(k)/L\,, \tag{4·6}$$

and is displayed in Fig. 3. In the actual calculation N is put to be a finite number, $N=1024\times100$. The spectrum forms a smooth curve and the large wave number behavior can be well explained by the following theoretical value derived in Appendix B:

$$\hat{S}(k) = (2\sqrt{2\pi a}/a^2)\exp(-4ak^2). \tag{4·7}$$

A qualitative property of the temporal correlation may be considered by calculating the power spectrum:

$$\tilde{S}(k, \omega) = \lim_{N\to\infty} \tilde{x}(k, \omega)\tilde{x}^*(k, \omega)/(LN) \tag{4·8}$$

Downloaded from https://academic.oup.com/ptp/article/72/5/885/1927016 by guest on 20 August 2022

with

$$\tilde{x}(k, \omega)=\sum_{n=1}^{N} e^{-i\omega n}\hat{x}_n(k). \tag{4·9}$$

The actual numerical calculation is carried out by using the FFT method and putting N equal to be 1024. Each figure shown in Fig. 4 is obtained by averaging the power spectrum over 100 times. Figures 4(a), (b), (c) and (d) show the power spectra for the wave numbers $k=0$, 40, 80 and 120, respectively. The peaks at $\omega=\pi$ and $\pi/2$ suggest the existence of the 2 cycle- and the 4 cycle-like structures in the time evolution of $\hat{x}_n(k)$. The small wave number behavior represented by Fig. 4(a) has a feature that the peak positions clearly deviate from π and $\pi/2$. This deviation becomes smaller as the value of a decreases and the strength of the chaotic behavior reduces. This feature may be one of characteristics of the chaos in the continuous system.

The same procedures as Figs. 1~4 are carried out for $a=3.8$ and the results are illustrated in Figs. 5~8. In Fig. 5 the space-time behavior is shown. The mappings, $x_n(r)\to x_{n+1}(r)$, at $r=0$, $L/4$, $L/2$, and $3L/4$, are shown in Figs. 6(a)~(d). The total number of points in each figure is 150. For this time interval these figures show the existence of periodic structure in the time evolution. However, this periodic structure cannot continue stationarily and is interrupted by the chaotic time sequence. After the chaotic time sequence the periodic

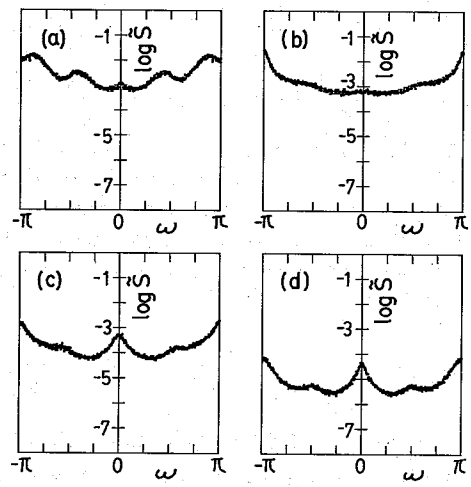

Fig. 4. The power spectra for $a=4.0$. The values of wave numbers are (a) $k=0$, (b) $k=40$, (c) $k=80$ and (d) $k=120$, respectively. The quantity $\tilde{S}$ denotes the power spectrum $\tilde{S}(k, \omega)$.

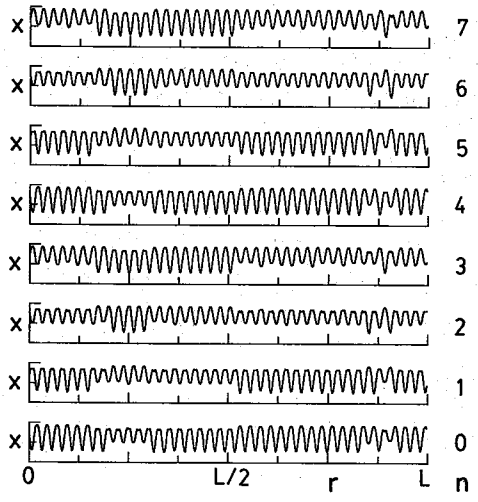

Fig. 5. The same as Fig. 1, but for $a=3.8$.

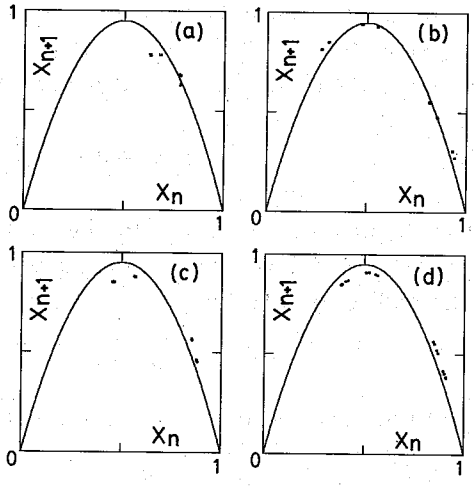

Fig. 6. The same as Fig. 2, but for $a=3.8$.

Downloaded from https://academic.oup.com/ptp/article/72/5/885/1927016 by guest on 20 August 2022

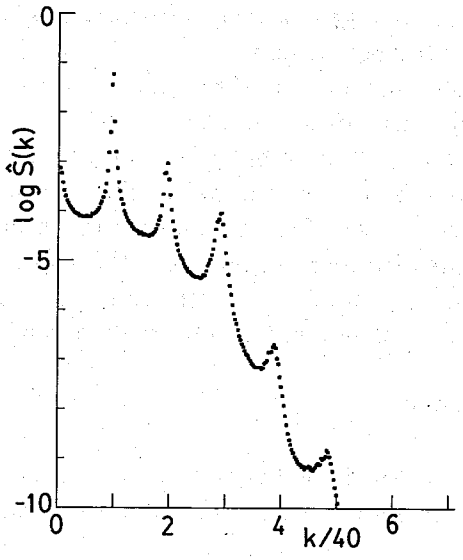

Fig. 7. The same as Fig. 3, but for $a=3.8$. In the figure only the results of the numerical calculation are shown.

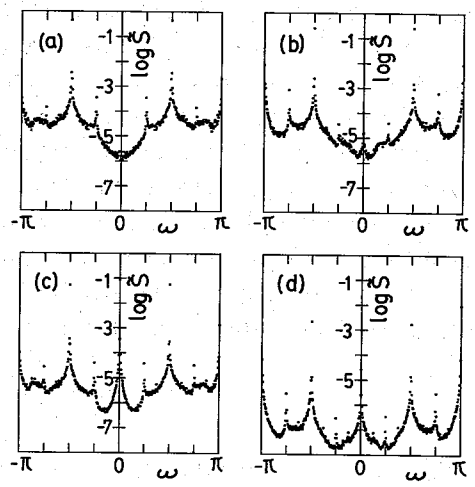

Fig. 8. The same as Fig. 4, but for $a=3.8$.

behavior is again recovered. The alternative appearance of the periodic and chaotic sequences is the characteristics of the intermittent chaos.[9] In Fig. 7 the equal time spectrum is shown. The spiky peaks correspond to the wavy patterns observed in Fig. 5. The power spectra for several k-values are shown in Fig. 8 and have the feature of 8-periodic like structure.

All the results in the present section do not depend on the choices of the mesh points and the system size. Theoretical understanding of the results may be possible by making use of the turbulence theories[10] and should be done separately.

§ 5. Summary and some remarks

In the present work we have proposed a mapping model for the description of the continuous system. The mapping model is obtained from the reaction-diffusion equation when the spatial variation of the state vector is not large.

As seen in §4, the present mapping model has the interesting properties of the chaotic continuous system. Intermittent behavior in the time evolution of the state variable reflects the intermittent spatial wavy pattern as is observed in Fig. 5. The intermittent behavior brings about the spiky peaks in the power spectra. The equal time spectra have also spiky peaks, which disappear as the strength of chaotic behavior becomes larger as a increases. The equal time spectrum for large wave numbers at $a=4$ is well described by the theoretical result obtained by a simple decoupling approximation. Since the renormalization effects are discarded in the theory, the agreement for small wave numbers is poor.

In the present work we considered the small a system for $L=2\pi$ which corresponds to the large size system with $a=1$. As the a value is increased with a fixed L, the bifurcation scheme appears and it finally leads to the uniform state. We get the sequence

Downloaded from https://academic.oup.com/ptp/article/72/5/885/1927016 by guest on 20 August 2022

of the chaotic and the periodic states in the bifurcation diagram. The bifurcation scheme is complicated because of the existence of the multi-basin structure.[11]

It is necessary to give a brief comment on the uniform state discussed in §3. In the chaotic "uniform" state the largest Lyapunov exponent of λ_k' is equal to $\lambda_L(=\lambda_0')$ and other Lyapunov exponents are all negative for $k\neq 0$. If a completely uniform state is realized, the attractor dimension of the continuous system is reduced to the one of the original mapping without diffusion. However the theories of fractal dimension[12] seem to suggest that the former dimension possibly deviates from the latter one. We will study this problem separately. The study of 2-dimensional mapping is interesting, associated with the problem of the attractor dimension. This problem will be also studied in future.

Acknowledgements

The authors would like to thank Professor H. Mori for his continuous encouragements. The study was partially supported by the Scientific Research Fund of the Ministry of Education, Science and Culture.

Appendix A

In this appendix we prove Eq. (2·4). The right-hand side of Eq. (2·2) can be expanded as

$$\boldsymbol{f}(\boldsymbol{x};\ t)+\sum_{m=1}^{\infty}\frac{(-Dt')^m}{m!}(\nabla^2)^m\boldsymbol{f}(\boldsymbol{x};\ t) \tag{A·1}$$

with $t'=t-t_n$. The spatial derivative in (A·1) is calculated as

$$\begin{aligned}(\nabla^2)^m f_\alpha(\boldsymbol{x};\ t)&=(\nabla^2)^{m-1}\nabla^2 f_\alpha(\boldsymbol{x};\ t)\\&=(\nabla^2)^{m-1}\left[\sum_\gamma\frac{\partial f_\alpha}{\partial x_\gamma}\nabla^2 x_\gamma+\sum_{\gamma,\beta,\delta}\frac{\partial^2 f_\alpha}{\partial x_\gamma\partial x_\delta}\cdot\frac{\partial x_\gamma}{\partial r_\beta}\cdot\frac{\partial x_\delta}{\partial r_\beta}\right]\\&=\sum_\gamma\frac{\partial f_\alpha}{\partial x_\gamma}(\nabla^2)^m x_\gamma+O(|\delta\boldsymbol{x}|^2),\end{aligned} \tag{A·2}$$

where f_α, x_γ and r_β are the α, γ, β components of $\boldsymbol{f}$, $\boldsymbol{x}$, and the position vector $\boldsymbol{r}$, respectively. The quantity $|\delta\boldsymbol{x}|$ defined by

$$|\delta\boldsymbol{x}|=l\sqrt{\overline{\nabla x_\alpha}} \tag{A·3}$$

with $l=\sqrt{DT}$ is the representative value of $l\nabla_\beta x_\alpha$, $l^2\nabla_\beta\nabla_\gamma x_\alpha$, $l^3\nabla_\beta\nabla_\gamma\nabla_\delta x_\alpha$, and so on, ($\nabla_\beta\equiv\partial/\partial r_\beta$), and is assumed to be small, where the notation $\overline{(\cdots)}$ denotes the spatial average. Therefore, Eq. (A·1) (its α component) becomes

$$f_\alpha(x;\ t)-\sum_\gamma\frac{\partial f_\alpha}{\partial x_\gamma}[1-\exp(-D\nabla^2 t')]x_\gamma+O(|\delta\boldsymbol{x}|^2). \tag{A·4}$$

On the other hand, from the definition of $\boldsymbol{y}$ we have

$$y_\gamma=\exp(-D\nabla^2 t')x_\gamma=x_\gamma-[1-\exp(-D\nabla^2 t')]x_\gamma. \tag{A·5}$$

Thus up to the first order in $|\delta\boldsymbol{x}|$ we get the expansion

Downloaded from https://academic.oup.com/ptp/article/72/5/885/1927016 by guest on 20 August 2022

$$f_a(\boldsymbol{y};\ t)=f_a(\boldsymbol{x};\ t)-\sum_\gamma \frac{\partial f_a}{\partial x_\gamma}[1-\exp(-D\nabla^2 t')]x_\gamma+O(|\delta\boldsymbol{x}|^2). \tag{A·6}$$

From the comparison of (A·4) with (A·6) we finally obtain the relation

$$\dot{y}_a=f_a(\boldsymbol{y};\ t)+O(|\delta\boldsymbol{y}|^2),$$

where we have used $|\delta\boldsymbol{x}|\sim|\delta\boldsymbol{y}|$.

Appendix B

We start with the mapping (4·1). The quantity $x_n(r)$ is divided into two parts:

$$x_n(r)=\bar{x}_n+\xi_n\,, \tag{B·1}$$

where $\bar{x}_n$ is the spatial average of $x_n(r)$ and ξ_n is the deviation from it. Correspondingly, Eq. (4·1) is written as

$$\bar{x}_{n+1}=a\Big[\bar{x}_n(1-\bar{x}_n)-L^{-1}\int_0^L \xi_n{}^2 dr\Big], \tag{B·2}$$

$$\hat{\xi}_{n+1}(k)=ae^{-\alpha k^2}[(1-2\bar{x}_n)\hat{\xi}_n(k)-(\xi_n{}^2)_k], \tag{B·3}$$

where

$$\hat{\xi}_n(k)=\int_0^L e^{ikr}\xi_n(r)dr\,, \tag{B·4}$$

$$(\xi_n{}^2)_k=L^{-1}\sum_{k'}\hat{\xi}_n(k-k')\hat{\xi}_n(k'). \tag{B·5}$$

The equal time spectrum is now given by

$$\hat{S}(k)=\int_0^L e^{ikr}\langle\xi_n(r)\xi_n(0)\rangle dr\,, \tag{B·6}$$

where the brackets denote an ensemble average and the spatial homogeneity of system is assumed.

By using (B·3) and applying a gaussian decoupling approximation a simple manipulation yields

$$\hat{S}(k)=a^2e^{-2\alpha k^2}\Big[\langle(1-2\bar{x}_n)^2\rangle\hat{S}(k)+\frac{2}{L}\sum_{k'}\hat{S}(k-k')\hat{S}(k')\Big]. \tag{B·7}$$

For $\alpha k^2\gg 1$ the first term of the right-hand side can be neglected and we get

$$\hat{S}(k)=\pi^{-1}a^2e^{-2\alpha k^2}\int_{-\infty}^{\infty}\hat{S}(k-k')\hat{S}(k')dk'\,, \tag{B·8}$$

where the summation over the wave number is replaced by the integral. This replacement can be justified for $\alpha(2\pi/L)^2\ll 1$. Equation (B·8) can be solved by assuming the following form:

$$\hat{S}(k)=A\exp(-\Gamma k^2). \tag{B·9}$$

The constants A and Γ can be easily determined as

Downloaded from https://academic.oup.com/ptp/article/72/5/885/1927016 by guest on 20 August 2022

$$\Gamma=4a, \qquad A=2\sqrt{2\pi a}/a^2 .$$

References

1) R. M. May and G. F. Oster, The American Naturalist **110** (1976), 573.
2) J. -P. Eckmann, Rev. Mod. Phys. **53** (1981), 643.
   H. L. Swinney, Physica **7D** (1983), 3.
3) G. Rowlands, J. of Phys. **A16** (1983), 585.
   A. H. Fowler and M. J. McGuinness, Physica **5D** (1982), 149.
   D. Broomhead et al., Phys. Lett. **84A** (1981), 229.
4) T. Yamada and H. Fujisaka, Prog. Theor. Phys. **70** (1983), 1240.
5) K. Kaneko, Prog. Theor. Phys. **69** (1983), 1427.
   J. M. Yuan et al., Phys. Rev. **A28** (1983), 1662.
   Y. Gu et al., Phys. Rev. Lett. **52** (1984), 701.
6) R. J. Deissler, Phys. Lett. **100A** (1984), 451.
   K. Kaneko, Prog. Theor. Phys. **72** (1984), 480.
7) Y. Kuramoto and T. Yamada, Prog. Theor. Phys. **56** (1976), 679.
   K. Nozaki and N. Bekki, Phys. Rev. Lett. **51** (1983), 2171.
8) H. Fujisaka and T. Yamada, Prog. Theor. Phys. **69** (1983), 32.
9) P. Manneville and Y. Pomeau, Physica **1D** (1980), 219.
   U. Frisch and R. Morf, Phys. Rev. **A23** (1981), 2673.
10) D. C. Leslie, Rep. Prog. Phys. **36** (1973), 1365.
11) S. Takesue and K. Kaneko, Prog. Theor. Phys. **71** (1984), 35.
12) For example, see J. D. Farmer, Physica **4D** (1982), 366.

Downloaded from https://academic.oup.com/ptp/article/72/5/885/1927016 by guest on 20 August 2022